Chaos Versus Noisy Periodicity: Alternative Hypotheses for Childhood Epidemics

L. F. Olsen and W. M. Schaffer

Whereas case rates for some childhood diseases (chickenpox) often vary according to an almost regular annual cycle, the incidence of more efficiently transmitted infections such as measles is more variable. Three hypotheses have been proposed to account for such fluctuations. (i) Irregular dynamics result from random shocks to systems with stable equilibria. (ii) The intrinsic dynamics correspond to biennial cycles that are subject to stochastic forcing. (iii) Aperiodic fluctuations are intrinsic to the epidemiology. Comparison of real world data and epidemiological models suggests that measles epidemics are inherently chaotic. Conversely, the extent to which chickenpox outbreaks approximate a yearly cycle depends inversely on the population size.

Especially in the physical sciences, the ubiquity of chaotic fluctuations is now well established (*1*). Fundamentally, chaos results from the action of nonlinear laws of motion. Because even very simple biological systems obey nonlinear equations, it should come as no surprise that there is also mounting evidence (*2*) for chaos in biology.

Recently it has been proposed that, in the absence of vaccination, recurrent epidemics of measles, poliomyelitis, and possibly mumps and rubella are chaotic (*3*). An alternative view (*4, 5*) is that these outbreaks represent periodic behavior in the presence of random perturbations. In particular, it has been suggested that the deterministic component of measles infections corresponds to an alternating pattern of high and low years (*5*).

We review here the dynamics of measles and chickenpox, the two infections for which we have been able to gather the most information. In detail, we study monthly case reports from eight large North American and European cities and two small islands. To analyze the data, we use traditional methods of spectral analysis as well as more recently developed techniques from nonlinear dynamics. We further compare incidence patterns for the real world infections with a standard epidemiological model, the so-called "SEIR" equations. The name is an acronym for Susceptible-Exposed-Infectious-Recovered, these being the categories into which the host population is divided. In particular, we consider the effects of seasonal variations in transmission and random perturbations. Our analyses suggest that, for large populations, temporal changes in chickenpox incidence are best explained as a noisy annual cycle. Conversely, variations in the incidence of measles exhibit the field marks of chaos. Finally, we predict and find erratic dynamics for both diseases in the case of small populations.

L. F. Olsen is in the Department of Biochemistry, Odense University, Campusvej 55, DK-5230 Odense M, Denmark. W. M. Schaffer is in the Department of Ecology and Evolutionary Biology, University of Arizona, Tucson, AZ 85721.

Case Reports for Chickenpox and Measles

Figure 1 (small boxes at upper left) shows monthly case reports of chickenpox and measles in New York City and on the Danish island of Bornholm for periods of 11 to 43 years (*6*). New York has a population of several million, whereas the inhabitants of Bornholm number about 50,000. For New York, the chickenpox data suggest an annual cycle perturbed by noise; for Bornholm, the time series is more irregular. In the case of measles, the data suggest yearly outbreaks of varying amplitude (with an apparent high-low biennial cycle from 1944 on) in New York and a more highly erratic pattern on Bornholm.

These conclusions are confirmed by the autocorrelation functions and power spectra, which are shown in the same figure (small boxes, lower left; main parts of each diagram). For chickenpox in New York, there is a single spectral peak corresponding to 1 cycle per year (cpy). In contrast, the Bornholm chickenpox data show peaks at 0.3 and 1.0 cpy emerging out of a noisy background that accounts for most of the variation. Both sets of measles data show multiple peaks. For New York, the major peak corresponds to an annual oscillation, and there is a subsidiary peak at 0.41 cpy. For Bornholm, the dominant peak corresponds to a period of 4 years.

Elsewhere (*7–9*) we have presented power spectra for other historical data sets: chickenpox in Copenhagen (Denmark), Milwaukee, and St. Louis and measles in Aberdeen (Scotland), Baltimore, Copenhagen, Detroit, Milwaukee, and St. Louis. In all cases, chickenpox exhibits a single spectral peak corresponding to the annual cycle. Measles epidemics are another matter. With the exception of the data for Aberdeen, each data set has two peaks: the first at 1.0 cpy, and the second in the region 0.34 to 0.46 cpy. Combining these results with the evidence in Fig. 1 suggests three conclusions. First, in large cities, outbreaks of measles epidemics are more irregular than outbreaks of chickenpox epidemics. Second, the overall patterns of both chickenpox and measles infections exhibit relatively little variation among large cities. Third, pronounced differences are observed when one compares large populations with small. These results accord with the writings of Anderson and May (*10*), who stress that, of the two diseases, measles is the more easily transmitted. They are also in agreement with the work of Bartlett (*11*), who was among the first to suggest that population size and isolation are important factors in shaping patterns of infection. Note that there is an interaction between population size and transmission efficiency. Measles is more highly infectious and therefore more liable to "burn itself out" in small populations (*12*).

Epidemiological Models

Here we compare real world epidemics with mathematical models. Specifically, we study the SEIR equations (*10, 13*), which divide the host population into four categories. One assumes that individuals enter the population at birth as susceptibles (S) and exit by death or by emigration. A susceptible becomes exposed (E) by contact with one or more individuals capable of transmitting the disease. Such individuals are called infectives (I). After a characteristic latency period, exposed individuals themselves become infective and later immune or recovered (R). For childhood diseases, immunity is permanent and recovered individuals do not revert to the susceptible class.

The SEIR model is most simply expressed as a set of four nonlinear differential equations:

$$dS/dt = m(N - S) - bSI$$

$$dE/dt = bSI - (m + a)E$$

$$dI/dt = aE - (m + g)I$$

$$dR/dt = gI - mR \quad (1)$$

of which one need only keep track of the first three. Typically, the population size, N, is assumed constant and normalized to 1, in which case, the state variables are expressed as proportions with $S + E + I + R = 1$. Average life expectancy is given by $1/m$, and $1/a$ and $1/g$ are, respectively, the mean latency and infectious periods; b is the effective contact rate, the average fraction of susceptibles contacted by a single infective, which themselves contract the infection.

Values of m, a, and g appropriate for various locales and diseases can be obtained directly from census data (in the case of m) and the medical literature (in the case of a and g). However, the contact rate, b, must be estimated indirectly from the average age of infection as calculated from age-specific serological profiles (*10, 13*).

When the parameters m, a, b, and g are held constant, the solution of Eq. 1 is a weakly damped oscillation. This is inconsistent with the observation of recurrent epidemics in real world populations. There are two possible modifications of the basic SEIR model that lead to sustained and, for measles parameters, irregular dynamics. Both were discussed by Bartlett (*11, 14*). The first modification is to perturb the equations with noise. Alternatively, one can introduce seasonal variations in the contact rate (*15, 16*). Several factors may induce seasonally varying transmission rates: the assembling and dispersion of schoolchildren at the beginning and end of term and changes in the virulence or viability of the pathogen resulting, due to variations in the weather (*10*).

To model the seasonal component, we replace the constant b in Eq. 1 by a time-dependent expression such as

$$b(t) = b_0(1 + b_1 \cos 2\pi t) \quad (2)$$

where b_0 is the average contact rate and b_1 is the seasonal component (*13*). Choosing values of a, g, and b_0 appropriate for chickenpox yields a simple annual cycle for all values of b_1 in the interval $0 < b_1 \leq 0.3$. This result agrees with the data obtained from New York City and other large cities (*3, 8, 9*). Repeating the calculations but using parameter values appropriate for measles yields a very different result. Specifically, one finds that qualitatively different dynamics obtain for different values of b_1. Thus, for $b_1 < 0.1$, one observes a simple annual cycle. At values of b_1 around 0.2, the dynamics change to a 2-year cycle. Further increases in seasonality induce successive period-doubling bifurcations, until around $b_1 \approx 0.28$ the solutions become chaotic (*7, 17*). Aron and Schwartz (*17*) have emphasized that, even after the transition to chaos, one continues to observe a seemingly regular alternation of high and low years. However, shortly thereafter, the pattern breaks down and there is an abrupt transition to more erratic fluctuations (*7, 9*) reminiscent of the outbreaks observed in New York City before 1945 (Fig. 1C). Thus, for both chickenpox and measles, the SEIR model with seasonal variations in contact rate can generate time series that resemble historical data (*8, 9*).

Other workers have argued that an estimate for β_1 around 0.28 for measles is too high and that the dynamics of this disease are better explained by a biennial cycle in the presence of noise (*4, 5*). Adding noise to the SEIR equations with measles parameters and choosing b_1 in the interval $0.2 < b_1 < 0.28$ yields incidence rates that also resemble those observed in nature. Because noise is always

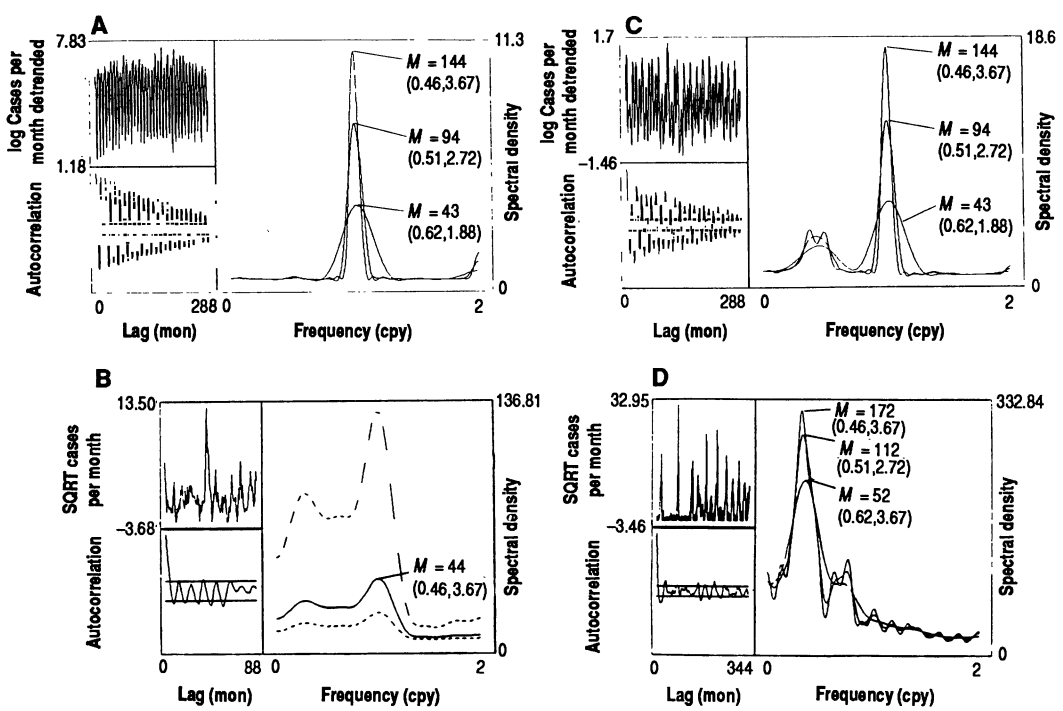

Fig. 1. Monthly notifications (upper left), autocorrelation functions (lower left), and power spectra (right) computed from monthly notifications of (**A**) chickenpox in New York, 1928 to 1963; (**B**) chickenpox in Bornholm, 1938 to 1948; (**C**) measles in New York, 1928 to 1963; and (**D**) measles in Bornholm, 1925 to 1967; SQRT, square root; mon, months. Smoothed spectra were estimated, using a Tukey window with M lags. The numbers in parentheses are the upper and lower multiplicative confidence intervals.

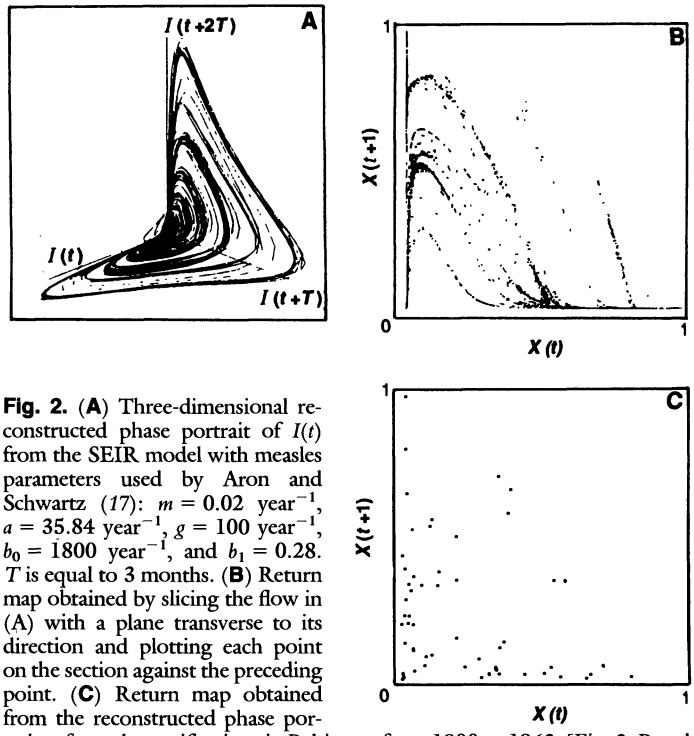

Fig. 2. (**A**) Three-dimensional reconstructed phase portrait of $I(t)$ from the SEIR model with measles parameters used by Aron and Schwartz (*17*): $m = 0.02$ year^{-1}, $a = 35.84$ year^{-1}, $g = 100$ year^{-1}, $b_0 = 1800$ year^{-1}, and $b_1 = 0.28$. T is equal to 3 months. (**B**) Return map obtained by slicing the flow in (A) with a plane transverse to its direction and plotting each point on the section against the preceding point. (**C**) Return map obtained from the reconstructed phase portraits of measles notifications in Baltimore from 1900 to 1963. [Fig. 2, B and C, is reprinted from (*22*) with permission of Academic Computing Publications, Inc.]

present in real systems, we conclude that simply inspecting the time series does not allow one to discriminate between chaos and noise-perturbed periodicity.

Reconstructed Trajectories and Return Maps

One way of detecting deterministic structure in a time series is to reconstruct motion in the phase space as prescribed by Takens (*18, 19*). For epidemiological data (case numbers), the value of $I(t)$ is lagged against itself, using a fixed time delay T, and the resulting points are plotted in the coordinate space, $I(t)$ versus $I(t + T)$, versus $I(t + 2T)$, ... As discussed, for example, by Broomhead and King (*20*), provided that one uses enough embedding dimensions, the new trajectory faithfully reproduces the dynamical properties of the original.

Figure 2A shows a three-dimensional reconstructed phase portrait for a typical realization of the SEIR model with measles parameters and $b_1 = 0.28$. The trajectory appears to pivot on a conical surface. Slicing the orbit with a plane transverse to the flow yields a nearly one-dimensional section, and a plot of each point on the section against the preceding point yields a return map (Fig. 2B). Effectively, this gives the relation of next year's cases to the current year's. In the present case, the return map exhibits a well-defined, though certainly not unique, relation between successive points on the section. Figure 2C displays a return map computed from data for the city of Baltimore and its environs. Taking into account the relative paucity of data for the real world example, one is nonetheless struck by the overall similarity of Fig. 2C to Fig. 2B. Applying this procedure to other historical data yields similar maps (*8, 9, 21, 22*).

Returning to the SEIR equations, for which one can compute as many points as needed, we note that the return map is in fact a "fractal," because successive magnifications of small pieces reveal a fine structure similar to that of the original (*23*). Interestingly and despite the lack of uniqueness, most points on the map can be predicted from the preceding pair. That is, if we label points in temporal sequence, it is true for most X_i that $X_{i+1} = F(X_i, X_{i-1})$, with monotonic dependence on X_{i-1} (Fig. 3).

More Fingerprints of Chaos

In attempting to assess the relative plausibility of the various hypotheses put forward to account for real world epidemics, it is important that one go beyond the qualitative information contained in pictures such as Fig. 2. Recall that chaotic systems exhibit a property called "sensitivity to initial conditions" (*24*). By this it is meant that nearby trajectories diverge and that the divergence is, on the average, exponentially fast. Trajectorial divergence in nonlinear systems such as the SEIR model is quantified by the maximum Lyapunov characteristic exponent (LCEs) (*25, 26*). LCEs are nothing more than generalized eigenvalues averaged over an attractor. Usually, they are expressed as bits per unit time. In the absence of random perturbations, one or more positive exponents imply that orbits separate exponentially and hence that the motion is chaotic. For the SEIR equations, there is a single positive exponent, λ_1, which can be estimated either directly from the equations or from the reconstructed trajectory (*26*). For measles parameters and $b_1 = 0.28$, we obtained from the equations $\lambda_1 = 0.48$ bit per year (bpy). This compares favorably with estimates for actual epidemics (*8, 9, 21*). For eight First World cities, λ_1 ranged from 0.3 to 0.7 bpy.

For chickenpox parameters, the SEIR model yields a periodic orbit, and $\lambda_1 = 0$. This result does not square with estimates for real world chickenpox epidemics which ranged from 0.12 to 0.32 bpy. To resolve this discrepancy, we repeated the simulations with small amounts of multiplicative noise. This time, we estimated λ_1 as 0.19 bpy when using chickenpox parameters and 0.55 bpy when using the measles parameters. We conclude that it is easy to find noise levels for which the SEIR model mimics real world behavior. Of greater importance (see below) is the fact that random perturbations have a more pronounced effect on simulated chickenpox epidemics (periodic dynamics) than on the measles simulations which are chaotic.

To further explore the effect of noise on the positive LCE, we have studied the SEIR model with measles parameters and different values of b_1 in the presence of Gaussian noise (Fig. 4A). For values of b_1 less than 0.2 and with the noise level at 1%, the estimated values of λ_1 were substantially less than estimates for eight real world cities. For the same values of b_1 but with the noise level set to 2%, the confidence limits for the simulations partially overlap the data. Far better agreement, however, is obtained for all three noise levels (0%, 1%, and 2%) if we take $b_1 \approx 0.28$, in which case the simulations and the data are indistinguishable.

Another way of characterizing a dynamical system is to compute its dimension (*27*). The dimension of a time series measures the complexity of the signal by providing an estimate of the amount of information needed to specify the position of a point in the state space.

We have computed the correlation dimension, D_C (*28*), for the historical chickenpox and measles data sets and for the SEIR model with chickenpox and measles parameters. The results are listed in Table 1 (*8, 9, 21*). In the presence of small noise levels, there is good agreement between the chickenpox simulations and the historical data. The same is true for measles. As in the case of the maximum LCE, noise has a dramatic effect on the dimension of chickenpox simulations but virtually no effect when the parameters are set to values appropriate for measles. It is also worth noting that the differences in dimension between the two diseases are consistent with differences in the return maps. Specifically, chickenpox has a

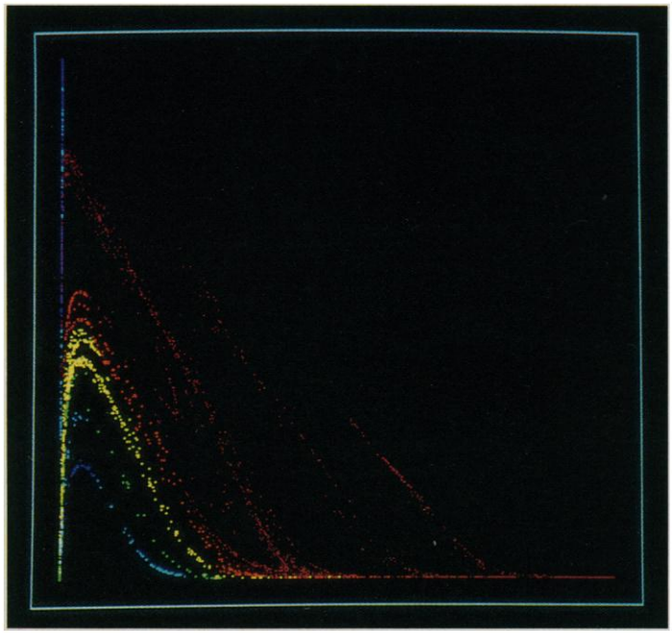

Fig. 3. Return map for the SEIR equations with parameter values appropriate for measles and $b_1 = 0.28$. X_{i+1} plotted against X_i with color-coding by X_{i-1}. For most values of X_i, X_{i+1} declines monotonically with increasing X_{i-1}; for example, all else being equal, a large outbreak in the previous year reduces the number of infections next year. Red indicates a low value of X_{i-1}; violet, a high value. For interpretation of the other colors, follow the visible spectrum.

Table 1. Correlation dimensions for chickenpox and measles. For data sources, see (*6*).

Community (dates)		Community size	Disease	
			Chick-enpox	Measles
Faroe Islands	(1912–1940)	22,500	—	1.73
Bornholm	(1925–1968)	47,000	—	2.33
Aberdeen	(1883–1902)	165,000	—	2.56
Copenhagen	(1927–1967)	660,000	3.38	3.07
Baltimore	(1900–1927)	750,000	—	2.34
Milwaukee	(1916–1965)	775,000	3.25	2.57
Baltimore County	(1928–1963)	1,285,000	—	2.42
St. Louis	(1934–1954)	1,620,000	2.76	2.22
Detroit	(1920–1962)	2,525,000	—	2.43
New York	(1927–1963)	9,235,000	3.33	2.68
SEIR equations			1.00	2.52
SEIR equations + 2% noise			3.41	2.47

higher dimension than measles and a return map (not shown) that resembles a random scatter of points (*3, 8, 9*).

Finally, we computed correlation dimensions for different values of b_1 and varying noise levels (Fig. 4B). For values of $b_1 \leq 0.23$, where the unperturbed dynamics correspond to an annual or a biennial cycle, the correlation dimensions estimated for the simulations are consistently higher than the estimates for the historical data. Conversely, in the region where the dynamics are chaotic, agreement between the model and real epidemics is excellent.

In comparing Fig. 4, A and B, we note that dimension estimates appear to provide a more consistent characterization of the dynamics than the maximal LCE. This finding is in keeping with the experience of other investigators who have worked with short time series (*29*).

Monte Carlo Simulations

In order to reproduce the historical chickenpox data by the SEIR model, it is necessary to add noise to the simulations. The question arises as to how much noise one should add. There are several sources of noise that undoubtedly distort epidemiological records. First of all, there are observational errors. The reporting rates for New York, Baltimore, and Copenhagen have been estimated as 12.5 to 50% for measles and 8 to 30% for chickenpox (3, 15). Although the reporting rates (*30*) for chickenpox (30%) and measles (50%) in Copenhagen were essentially constant from 1927 to 1967, there may still have been month-to-month fluctuations. Second, there are actual perturbations to the dynamics. These can result from changes in population size and birth and death rates, chance variations in the weather, and the random movement of infectives into and out of the population. Finally, there is an intrinsic probabilistic element that results from finite population size. Because the second and third factors affect the actual dynamics, they can induce what amount to "noise-induced bifurcations" and hence changes in dimension and rates of trajectorial separation. Conversely, the effects of (small) observational error will only show up at small length scales.

With regard to the consequences of finite population size, the transmission of infectious diseases follows probability rules (*11, 14, 31*). In Eq. 1, the latency and infectious periods and the contact rate are all average measures and may vary from one individual to another. Furthermore, actual transitions are discrete rather than continuous. For example, the birth of a susceptible increases the population size by one individual; when that person is exposed, the group of susceptibles is reduced by one, the group of exposed increased by one, and so forth.

To investigate the effects of finite populations, we reformulated

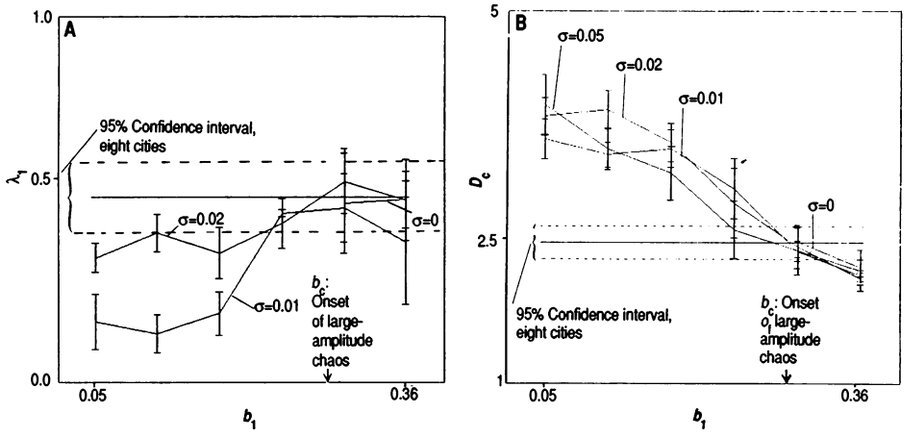

Fig. 4. Maximum Lyapunov exponents (**A**) and correlation dimensions (**B**) as a function of b_1 of simulations of the SEIR model with measles parameters and different levels of noise, σ. For each combination of parameters, ten 50-year replicates were analyzed. Error bars give 95% confidence intervals for each experiment.

the SEIR equations as a Monte Carlo process (*8*). Figure 5 shows Monte Carlo simulations (time series and spectra) of chickenpox and measles in populations with 5 million and 50,000 individuals. For small populations, the simulations resemble the data from Bornholm (Fig. 1, B and D); for large populations, the simulated data are similar to actual epidemics in New York (Fig. 1, A and C) (*32*). These results suggest that much of the noise in the historical data may result from what amounts to sampling error. For very large populations, the Monte Carlo simulations induce dynamical behaviors identical to those obtained from the differential equations (*33*).

We repeated the Monte Carlo calculations of measles epidemics for other population sizes and with different levels of seasonality. For each data set, we computed the correlation dimension (Fig. 6). For populations with 100,000 inhabitants or less, all values of b_1 yield essentially the same dimension. However, as the population size grows beyond 200,000, it becomes possible to distinguish different levels of seasonality. In Fig. 6, we also display the estimated correlation dimensions for the historical data. Dimensions for real cities are in good agreement with the Monte Carlo simulations only if we assume that $b_1 \geq 0.28$, that is, that the dynamics are intrinsically chaotic.

These results further accord with the notion of "critical community size," which is the minimum population size for which a disease will not die out as a result of chance extinction. As noted by Bartlett (*11*) and others, recurrent measles epidemics in small isolated populations are controlled by extinction and chance introduction, factors that are independent of b_1 and hence of the long-term deterministic dynamics. For larger populations, chance extinctions are less probable, in which case patterns of infection do depend on b_1. For measles, the critical community size has been estimated to be around 250,000 (*11, 14, 34*), which is roughly the point at which the curves in Fig. 6 diverge.

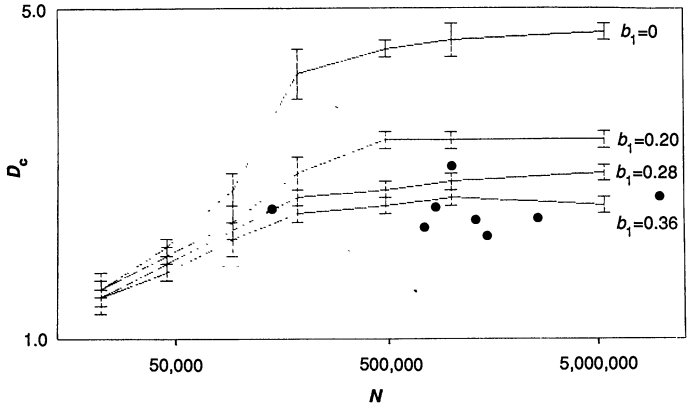

Fig. 6. Effect of the population size on the correlation dimension of Monte Carlo simulations with measles parameters and different values of b_1. Replicates and error bars are as in Fig. 4. The solid circles are the correlation dimensions calculated for the ten historical measles data sets.

Conclusions

The foregoing analysis suggests that chickenpox epidemics in large populations correspond to noisy limit cycles—periodic orbits, with a period of 1 year. For measles epidemics, we have considered three hypotheses:

1) The fluctuations have a probabilistic origin (*11, 14*).

2) The dynamics correspond to a high-low 2-year cycle perturbed by noise (*4, 5, 10, 17, 35*).

3) The fluctuations are chaotic (*3, 4, 7–9, 21, 36*).

Hypotheses 2 and 3 require that the transmission rate is seasonally dependent, whereas hypothesis 1 requires no seasonality. Our analyses suggest that, for large populations, seasonality is necessary to account for the estimates of dynamical quantities such as LCEs and correlation dimensions. However, for small populations, the dynamics accord with chance extinction and immigration, hypothesis 1. As for hypotheses 2 and 3, the critical point is the magnitude of the seasonal component, b_1 (*4*). This parameter was estimated by London and Yorke (*15*) to be around 0.25. Other workers (*5*) suggested an upper limit of 0.2, which is in the region where the SEIR model shows a biennial cycle. Our own studies suggest that the dynamics of the historical data sets correspond to those of the SEIR model when $0.28 \leq b_1 \leq 0.36$. We therefore conclude either

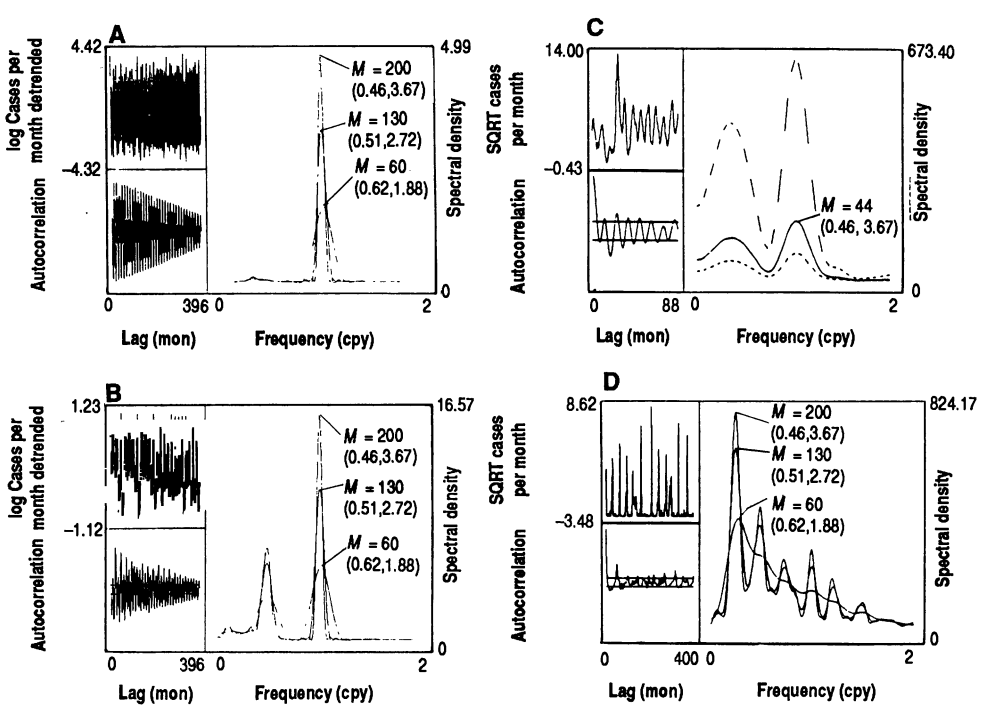

Fig. 5. Monte Carlo simulations of (**A**) chickenpox and (**B**) measles for populations of 5 million individuals; Monte Carlo simulations of (**C**) chickenpox and (**D**) measles for populations of 50,000 individuals.

that the claim for $b_1 = 0.2$ is wrong or that the SEIR model is an overidealization and that more realistic models would show chaos at lower values of b_1.

Our analyses also argue against the likelihood that factors such as changes in the population size or other parameters could result in fluctuations similar to those observed for measles epidemics. Specifically, estimated correlation dimensions were independent of the population size for populations of more than 200,000 (Fig. 6). In sum, the most plausible interpretation of the historical data is that, before mass immunization, measles infections in large communities were chaotic. This interpretation implies that fluctuations in incidence have a large deterministic component and are, at least in principle, subject to nonlinear forecasting techniques such as those developed by Farmer and Sidorowich (*37*). However, these conclusions are entirely within the context of the SEIR model. It remains possible that other models, in which chaos does not occur, can give equally good or even better fits to the data.

REFERENCES AND NOTES

1. See, for example, H. G. Schuster, *Deterministic Chaos, an Introduction* (VCH Verlagesellschaft, Weinheim, West Germany, ed. 2, 1988); B. L. Hao, Ed., *Chaos* (World Scientific, Singapore, 1984); P. Bergé, Y. Pomeau, C. Vidal, *Order Within Chaos* (Wiley, New York, 1984); P. Cvitanović, Ed., *Universality in Chaos* (Adam Hilger, Bristol, United Kingdom, 1984).
2. See, for example, L. Glass and M. C. Mackey, *From Clocks to Chaos, The Rhythms of Life* (Princeton Univ. Press, Princeton, NJ, 1988); H. Degn, A. V. Holden, L. F. Olsen, Eds., *Chaos in Biological Systems* [North Atlantic Treaty Organizaton Advanced Studies Institutes Series: Series A, Life Sciences (Plenum, New York, 1987), vol. 138]; L. F. Olsen and H. Degn, *Q. Rev. Biophys.* **18**, 165 (1985); W. M. Schaffer and M. Kot, *BioScience* **35**, 342 (1985); W. M. Schaffer, *IMA (Inst. Math. Appl.) J. Math. Appl. Med. Biol.* **2**, 221 (1985).
3. W. M. Schaffer and M. Kot, *J. Theor. Biol.* **112**, 403 (1985); L. F. Olsen, *Math. Comput. Modelling* **10**, 155 (1988).
4. R. Pool, *Science* **243**, 25 (1989).
5. I. B. Schwartz, in *Biomedical Modelling and Simulation*, J. Eisenfeld and D. S. Levine, Eds. (Baltzer, Berlin, 1989), p. 201.
6. Data were obtained from the following sources: Aberdeen, Scotland, and Baltimore, MD, Anderson, Grenfell, and May (*35*), courtesy of B. Grenfell; Bornholm, Copenhagen, and the Faroe Islands, Medical Report for the Kingdom of Denmark, 1927–1968, National Health Service of Denmark, Copenhagen; County of Baltimore, Yorke and London (*16*); New York City, Yorke and London (*16*); Detroit, Milwaukee, and St. Louis, Public Health offices of these cities. For discussions of the reliability and reporting frequencies, see below and London and Yorke (*15*) and Olsen *et al.* (*8*). Monthly cases of chickenpox were not reported for Bornholm before 1938 and after 1948. For the reconstructed maps and phase portraits only (data and simulations), monthly case reports were subjected to three-point smoothing and interpolated with cubic splines.
7. M. Kot, W. M. Schaffer, G. L. Truty, D. J. Graser, L. F. Olsen, *Ecol. Modelling* **43**, 75 (1988).
8. L. F. Olsen, G. L. Truty, W. M. Schaffer, *Theor. Popul. Biol.* **33**, 344 (1988).
9. W. M. Schaffer, L. F. Olsen, G. L. Truty, S. L. Fulmer, in *The Ubiquity of Chaos*, S. Krasner, Ed. (AAAS, Washington, DC, in press).
10. R. M. Anderson and R. M. May, *Science* **215**, 1053 (1982); R. M. Anderson, in *The Population Dynamics of Infectious Diseases: Theory and Applications*, R. M. Anderson, Ed. (Chapman and Hall, London, 1982), p. 1; R. M. Anderson and R. M. May, *J. Hyg. (London)* **94**, 365 (1985).
11. M. S. Bartlett, *Proc. Third Berkeley Symp. Math. Stat. Probab.* **4**, 81 (1956); *J. R. Statist. Soc. A* **120**, 48 (1957); *Stochastic Population Models in Ecology and Epidemiology* (Methuen, London, 1960).
12. Possibly *Herpes zoster* may further reduce the likelihood of chance extinctions in small populations by serving as a reservoir for future infections.
13. K. Dietz, *Lect. Notes Biomath.* **11**, 1 (1976).
14. N. T. J. Bailey, *The Mathematical Theory of Infectious Diseases and Its Applications* (Griffin, London, 1975).
15. W. P. London and J. A. Yorke, *Am. J. Epidemiol.* **98**, 453 (1973).
16. J. A. Yorke and W. P. London, *ibid.*, p. 469; J. A. Yorke, N. Nathanson, G. Pianigiani, J. Martin, *ibid.* **109**, 103 (1979); P. E. M. Fine and J. A. Clarkson, *Int. J. Epidemiol.* **11**, 5 (1982).
17. J. L. Aron and I. B. Schwartz [*J. Theor. Biol.* **110**, 665 (1984)] observed that there is a tradeoff between the average contact rate and the degree of seasonality. That is, the higher the mean rate, the smaller the amount of seasonal forcing required to induce period-doubling and ultimately chaos.
18. F. Takens, in *Dynamical Systems and Turbulence, Warwick*, D. A. Rand and L. S. Young, Eds. (Springer-Verlag, New York, 1981), p. 366.
19. N. H. Packard, J. P. Crutchfield, J. D. Farmer, R. S. Shaw, *Phys. Rev. Lett.* **45**, 712 (1980).
20. D. S. Broomhead and G. P. King, *Physica D* **20**, 217 (1986).
21. W. M. Schaffer, L. F. Olsen, G. L. Truty, S. L. Fulmer, D. J. Graser, in *From Chemical to Biological Organization*, M. Markus, S. C. Müller, G. Nicolis, Eds. (Springer-Verlag, Berlin, 1988), p. 331.
22. W. M. Schaffer and G. L. Truty, *Acad. Comput.* **2**, 34 (March-April 1988).
23. B. Mandelbrot, *The Fractal Geometry of Nature* (Freeman, San Francisco, 1982).
24. D. Ruelle, *Ann. N.Y. Acad. Sci.* **316**, 408 (1979).
25. R. Shaw, *Z. Naturforsch. Teil A* **36**, 80 (1981).
26. A. Wolf, in *Chaos*, A. V. Holden, Ed. (Manchester Univ. Press, Manchester, 1986), p. 273.
27. J. D. Farmer, E. Ott, J. A. Yorke, *Physica D* **7**, 153 (1983).
28. P. Grassberger and I. Procaccia, *ibid.* **9**, 189 (1983).
29. A. Wolf, J. B. Swift, H. L. Swinney, J. A. Vastano, *ibid.* **16**, 285 (1985). C. Sayers (personal communication to W.M.S.) has noted that LCEs provide a less reliable means of characterizing short time series than the correlation dimension.
30. Estimates of the reporting rate are based on the fact that 100% of a population acquires measles before the age of 20. Thus the reporting rate can be estimated as the total number of case reports in a 20-year period divided by the total number of newborns in the same period.
31. A. Cliff, P. Haggett, J. Ord, G. Versey, *Spatial Diffusion, an Historical Geography of Epidemics in an Island Community* (Cambridge Univ. Press, Cambridge, 1981).
32. The agreement is also quantitative. For example, considering the reporting rates of chickenpox and measles in Denmark, one would expect from the Monte Carlo simulations to observe peak values of 200 cases per month for chickenpox and 1,350 cases per month for measles on Bornholm. Considering the reporting rates for chickenpox and measles in New York, one would expect to see peak values of 3,800 cases per month for chickenpox and 10,500 cases per month for measles. Power spectra were also computed for measles on the Faroe Islands from 1927 to 1968. The spectra were similar to those obtained for measles on Bornholm. The population size of the Faroe Islands is about 25,000.
33. P. Lindblad and H. Degn, *Acta Chem. Scand.* **21**, 791 (1967).
34. F. L. Black, *J. Theor. Biol.* **11**, 207 (1966).
35. R. M. Anderson, B. T. Grenfell, R. M. May, *J. Hyg. (London)* **93**, 587 (1984).
36. F. Drepper, in *Ecodynamics*, W. Wolff, C.-J. Soeder, F. R. Drepper, Eds. (Springer-Verlag, Berlin, 1988), p. 319.
37. J. D. Farmer and J. Sidorowich, *Phys. Rev. Lett.* **59**,.845 (1987).

38. Research supported by the National Institutes of Health (U.S.A.), the Danish Natural Science Research Council, and North Atlantic Treaty Organization Scientific Affairs Division. G. Truty performed many of the computations. S. Fulmer and B. Smith prepared the graphs.